

RESONANT AND NONRESONANT ELECTRON CYCLOTRON HEATING AT  
DENSITIES ABOVE THE PLASMA CUT-OFF BY O-X-B-MODE  
CONVERSION AT W7-AS.

H.P. Laqua, V. Erckmann, H. J. Hartfuß, W7-AS Team  
Max-Planck-Institut für Plasmaphysik, EURATOM Ass.  
D-85748 Garching, FRG,

ECRH-Group  
Institut für Plasmaforschung, Univ. Stuttgart, D-70569 Stuttgart, FRG

H. Laqua  
Institut für Meß- und Regelungstechnik, Univ. Karlsruhe, D-76128 Karlsruhe, FRG

The O-X-B mode conversion process was proposed in 1973 [1] as a possibility to overcome the density limit for electron cyclotron resonance heating (ECRH). Here O, X, and B represent the ordinary, extraordinary and electron Bernstein mode. The essential part of this scheme is the conversion of the O-wave launched by an antenna from the low field side into an X-wave at the O-wave cut-off layer. This mode conversion requires an O-wave oblique launch near an optimal angle.

As shown in Fig. 1 the transverse refractive indices  $N_x$  of the O-wave and X-wave are connected at the optimal launch angle with a corresponding longitudinal (parallel  $B_0$ ) index  $N_{z,opt} = \sqrt{Y/(Y+1)}$  with  $Y = \omega_{ce}/\omega$  ( $\omega$  is the wave frequency,  $\omega_{ce}$  is the electron cyclotron frequency) without passing a region of evanescence ( $N_x^2 < 0$ ). For non-optimal launch an evanescent region always exists near the cut-off surface. The geometrical size of this evanescent region depends on the density scale length  $L = n_e / (\partial n_e / \partial x)$ , and a considerable fraction of the energy flux can be transmitted through this region, if  $L$  becomes small. The power transmission function  $T(N_y, N_z)$  is [2]

$$T(N_y, N_z) = \exp \left\{ -\pi k_0 L \sqrt{\frac{Y}{2}} \left[ 2(1+Y)(N_{z,opt} - N_z)^2 + N_y^2 \right] \right\},$$

where  $N_y$  and  $N_z$  are the poloidal and longitudinal components of the vacuum refractive index and  $k_0$  the wave number. This angular dependence ( $N_z$ -dependence) was used in the experiments to identify the O-X-conversion process. After the O-X-conversion the X-wave propagates then back to the upper hybrid resonance (UHR) layer where the refractive index of the X-wave is connected to that of the electron Bernstein waves (EBW) as shown in Fig. 1 and a complete conversion into EBW's may take place. The EBW's propagate then towards the plasma centre where they are absorbed near the electron cyclotron resonance layer or in the nonresonant case by collisional multiple pass damping.

In our calculations, additionally, we take into account that in a real plasma the conversion layer is not a smooth surface but is due to density fluctuations rough and wavy. This introduces a beam divergence much higher than the intrinsic one and can reduce the O-X-conversion considerably.

With a statistic description of the poloidal cut-off surface roughness (toroidal fluctuations were neglected), the probability density function of the poloidal component  $N_y$  (similar to a poloidal beam divergence)

$$p(N_y) = \frac{\lambda_y}{\sqrt{2\pi}\sigma_x} \exp\left(-\frac{N_y^2 \lambda_y^2}{(1-N_y^2)2\sigma_x^2}\right) \left(1-N_y^2\right)^{-\frac{3}{2}}$$

could be calculated as a function of the fluctuation amplitude standard deviation  $\sigma_x = L\tilde{n}_e/n_e$  ( $\tilde{n}_e/n_e$  is the relative fluctuation amplitude) and the poloidal correlation length  $\lambda_y$ . The modified power transmission function  $T_{mod}$  (O-X conversion efficiency) is then  $T_{mod}(N_z) = \int T(N_y, N_z) p(N_y) dN_y$ . In Fig. 2 the modified transmission is calculated as a function of the parameter  $k_0 L$  for five different relative density fluctuation amplitudes. In all calculations the poloidal correlation length was assumed to be 2 cm. It can be clearly seen that a significant heating efficiency is obtained only at a very small density scale length or a very low fluctuation amplitude. The flexibility of W7-AS allows to investigate both extreme cases, i.e. target plasmas with  $k_0 L \leq 10$  and with a relative density fluctuation amplitude of more than 20 % or peaked density profiles ( $k_0 L = 60$ ) with a very low relative fluctuation amplitude of less than 2%. For both cases, high conversion efficiencies were experimentally measured and O-X-B mode conversion for plasma heating could be clearly shown for the first time.

Two 70 GHz beams were launched into a neutral beam (NBI) sustained target plasma at resonant (1.25 T) and nonresonant (1.75 T, 2.0 T) magnetic fields. The launch angle of the incident O-mode polarised wave was varied at fixed heating power (220 kW). An example of the nonresonant case is shown in Fig. 3. The increase of the total stored plasma energy (from the diamagnetic signal) depends strongly on the launch angle, which is typical for the O-X-conversion process, and fits well to the calculation. Here the power transmission function was normalised to the maximum energy increase. The central density was  $1.5 \cdot 10^{20} \text{ m}^{-3}$ , which is more than twice the cut-off density, the central electron temperature was 500 eV. Heating at the plasma edge could be excluded since at the nonresonant magnetic field of 1.75T no electron cyclotron resonance exist inside the plasma. Due to technical limitation of the maximum launch angle, only the left part of the reduced transmission function could be proved experimentally.

In the X-B-conversion process near the UHR parametric instabilities are expected, which generate decay waves with frequencies of the incident pump wave  $\omega$  plus and minus the harmonics of the lower hybrid frequency  $\omega_{LH}$  and the lower hybrid (LH) wave itself. With the electron cyclotron emission (ECE) receiver a spectrum of the decay waves with maxima at  $\omega \pm n\omega_{LH}$  was measured for a resonant magnetic field of 1.25 T and is shown in Fig. 4. Note, that the pump wave is suppressed and the ECE-spectrum is clearly nonthermal since the density was twice the 70 GHz cut-off density. The low frequency LH-wave itself could be detected with a broad band loop antenna. A high degree of correlation between the high frequency decay waves and LH-wave was measured.

EBW's experience a cut-off layer ( $N \rightarrow 0$ ) at the upper hybrid resonance (UHR) surface (see Fig. 1), which in the nonresonant or higher harmonic ( $n > 1$ ) field totally encloses the inner plasma. The radiation is then trapped inside the plasma like in a hohlraum. The EBW is either

reflected at the UHR surface in the case of an oblique angle of incidence or is back converted to the X-wave which is converted again to the EBW at its next contact with the UHR. The only way that radiation can escape out of the Plasma is the small angular window for O-X- and X-O-conversion, respectively. In the absence of an electron cyclotron resonance in the plasma the EBW's may be absorbed due to finite plasma conductivity after some reflections at the UHR-layer. Nonresonant heating was clearly observed at magnetic fields up to 2.0 T. At the maximum field the plasma energy content increased by about 1.5 kJ compared to a similar discharge with NBI only (see Fig. 5). Two 70 GHz beams in O-mode polarisation (110 kW power each) were launched with an angle of  $40^\circ$  with respect to the perpendicular launch into a NBI (800 kW) sustained target plasma with a central density of  $1.6 \cdot 10^{20} \text{ m}^{-3}$  and a central temperature of 560 eV. More than 80% of the heating power was found in the plasma if the power scaling of the energy confinement ( $P^{-0.6}$ ) was taken into account. Thus O-X-B-heating turned out to be very efficient.

Ray-tracing calculation were performed with newly developed code in order to get a more detailed insight into the O-X-B-scheme. Density, temperature and magnetic field profiles similar to that of a typical neutral beam sustained W7-AS plasma were used for model calculations for a straight plasma cylinder. We use the nonrelativistic hot dielectric tensor with a correction for electron ion collisions given by Stix [3] and an isotropic electron temperature. The ray trajectory in the x-z-plane is shown in Fig. 6. The beam is launched from the low field side (LFS) and propagates through the cut-off, where it is converted into X-mode. Then it moves back to the UHR-layer, where the X-B-conversion takes place. The EBW's are absorbed near the cyclotron resonance at the plasma centre. A small fraction of the beam power is lost at the UHR due to finite plasma conductivity. The power deposition zone for resonant heating strongly depends on the magnetic field and the electron temperature, but central power deposition seems possible. In calculations for the nonresonant case more than 40% of the beam power is absorbed due to finite plasma conductivity after six passes through the plasma.

**In conclusion:** efficient O-X-B heating with 70 GHz electron cyclotron waves was clearly demonstrated for the first time for resonant and nonresonant fields at W7-AS. Both, the angular dependence of the O-X-conversion and the parametric instability which is typical for X-B-conversion could be experimentally verified. Density fluctuations at the O-X-conversion layer play a significant role in the O-X-B-process and need to be taken into account.

With a newly developed three dimensional ray-tracing code for EBW's and improved measurement techniques of the power deposition profiles further investigations of the O-X-B-heating are envisaged to explore the potential of resonant and nonresonant O-X-B-heating for routine high density operation.

## References

- [1] J.Preinhalter and V.Kopecký, J. Plasma Phys. 10 (1973) 1;
- [2] E.Mjølhus, J. Plasma Phys. 31 (1984) 7;
- [3] T.H.Stix: "THEORY OF PLASMA WAVES"; McGraw-Hill, 1962

Figures:

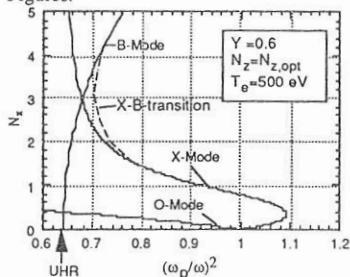


Fig. 1: Refractive index  $N_z$  versus  $\omega_p^2/\omega^2$  for the O-X-B conversion process. The transition represents the connection of the X-mode and B-mode due to the hot dielectric tensor.

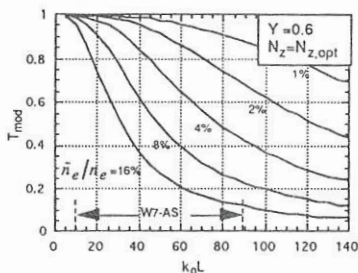


Fig. 2: Modified O-X-conversion in the presence of density fluctuations at the plasma cut-off layer versus normalised density scale length  $k_0 L$  for different relative fluctuation amplitudes.

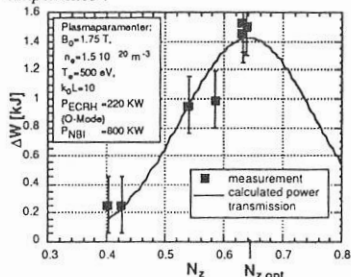


Fig. 3: Increase of the plasma energy content by O-X-B-heating versus the longitudinal vacuum refractive index  $N_z$  of the incident O-wave

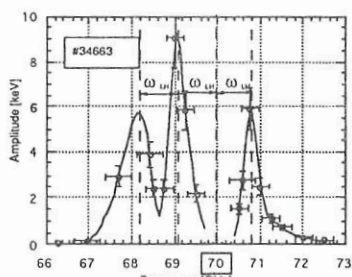


Fig. 4: High frequency spectrum of the parametric decay waves generated in the O-X-B-process. The incident wave frequency is 70 GHz and the LH frequency is about 900 MHz.

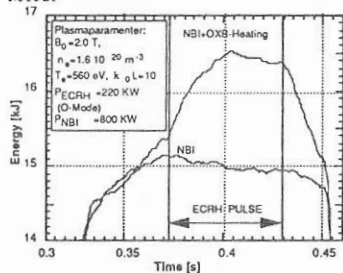


Fig. 5: Energy content (diamagnetic signal) of a NBI-discharge with and without nonresonant O-X-B-heating.

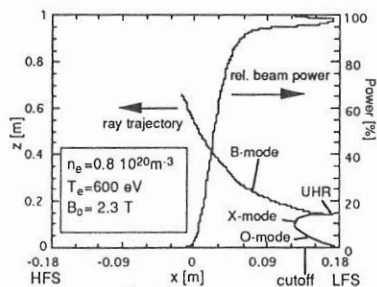


Fig. 6: Calculated ray trajectory in the  $x$ - $z$ -plane and relative beam power for resonant O-X-B-heating.